Insight into electric field-induced rupture mechanism of water-in-toluene emulsion films from a model system

Desislava Dimova, Stoyan Pisov, Nikolay Panchev, Miroslava Nedyalkova, Sergio Madurga, and Ana Proykova

Citation: The Journal of Chemical Physics **146**, 194703 (2017); doi: 10.1063/1.4983163
View online: https://doi.org/10.1063/1.4983163
View Table of Contents: http://aip.scitation.org/toc/jcp/146/19
Published by the American Institute of Physics

Insight into electric field-induced rupture mechanism of water-in-toluene emulsion films from a model system

Desislava Dimova,[1] Stoyan Pisov,[1,a)] Nikolay Panchev,[2,b)] Miroslava Nedyalkova,[3] Sergio Madurga,[4,c)] and Ana Proykova[1,d)]
[1]*Department of Atomic Physics, University of Sofia, Sofia, Bulgaria*
[2]*Institute of Physical Chemistry, Bulgarian Academy of Sciences, Sofia, Bulgaria*
[3]*Department of General and Inorganic Chemistry, University of Sofia, Sofia, Bulgaria*
[4]*Material Science and Physical Chemistry Department and IQTCUB, University of Barcelona, Barcelona, Spain*

(Received 26 January 2017; accepted 26 April 2017; published online 17 May 2017)

This paper presents a model, which we have designed to get insight into the development of electro-induced instability of a thin toluene emulsion film in contact with the saline aqueous phase. Molecular dynamics (MD) simulations demonstrate the role of charge accumulation in the toluene-film rupture induced by a DC electric field. Two ensembles—*NVT* and *NPT*—are used to determine the critical value of the external field at which the film ruptures, the charge distribution and capacitance of the thin film, number densities, and the film structure. The rupture mechanism as seen from this model is the following: in both *NVT* and *NPT* ensembles, *condenser plates*, where the charge density is maximal, are situated at the very border between the bulk aqueous (water) phase and the mixed layer. No ion penetration is observed within the toluene core, thus leaving all the distribution of charges within the mixed zone and the bulk phase that could be attributed to the formation of hydration shells. When the critical electric field is reached within a certain time after the field application, electric discharge occurs indicating the beginning of the rupturing process. The MD simulations indicate that the *NPT* ensemble predicts a value of the critical field that is closer to the experimental finding. *Published by AIP Publishing.* [http://dx.doi.org/10.1063/1.4983163]

I. INTRODUCTION

Water-in-oil emulsions are commonly formed during petroleum production and pose serious threats to installations and quality of the final product. The electrical phase separation has been used in the petroleum industry for separating water-in-crude oil dispersions by applying a high electric field onto the flowing emulsion to affect the flocculation and coalescence of dispersed water droplets.[1,2]

It has been realized that the emulsion is stabilized by a thin film formed between two drops when approaching each other. Thus, demulsification requires rupturing of this thin liquid film.

Generally, the main purpose of an applied electrical field is to promote contact between the drops and to help in drop–drop coalescence. Pulsed DC (direct current) and AC (alternative current) electric fields are preferred over constant DC fields for efficient coalescence. Recent studies have helped to clarify the important aspects of the process, such as partial coalescence and drop–drop non-coalescence, but key phenomena such as thin film breakup and chain formation are still unclear.[3] Despite the tremendous practical importance of enhanced coalescence, the mechanism of separation is not fully understood[4] beyond the perception that the electrical force facilitates the coalescence between small drops. This is due to basic non-understanding of the fundamental factors that lead to film (de)stabilization. Such factors are the following: (i) What are the reasons for obtaining stable organic films that prevent the coalescence of water droplets, i.e., how indigenous crude oil surfactants (like asphaltenes, resins, and naphtenates) stabilize the films on molecular level? (ii) What is the intimate structure of the film and mechanisms of film rupture? (iii) Once some clarity is gained regarding the stability reasons and film structure, what could be the optimum electric fields that should be applied for efficient phase separation, i.e., without causing disintegration of aqueous drops (emulsification at too high electric fields) and only coalescence? The subject is further complicated by the choice of proper molecular structure (amongst the thousands) of demulsifiers that are usually being used in combination with the electric grids.

The experimental results for electrical properties and the electric field-induced rupture of single thin films are scarce, which limits the comparison with computational results to several measurable quantities—pore formation and the critical voltage for film rupture. Anklam *et al.*[5] experimentally demonstrated that the electric-field induced pore formation was the reason for the break-up of emulsion films. Panchev *et al.*[6] developed a method allowing simultaneous investigation of a single water-in-oil emulsion film by both microinterferometry and electrical measurements. This method allows in a single experiment to measure the critical voltage of film rupture, the film thickness, the drainage rate, and the disjoining pressure laying the groundwork for computational studies.

a)Electronic mail: pisov@phys.uni-sofia.bg
b)Electronic mail: patcho75@yahoo.com
c)Electronic mail: s.madurga@ub.edu
d)Electronic mail: anap@phys.uni-sofia.bg

It is worth mentioning that so far there is almost complete lack of understanding of the intimate structural details of the crude petroleum-like films. Therefore, the current industrial practice of utilization of chemical additives in combination with electric field applications has for long time been widely viewed as a "work of art." To help in understanding the inherent processes, computational models were designed to simulate the coalescence of droplets under realistic experimental conditions. The molecular dynamics (MD) method is a useful tool for the purpose. Koplik and Banavar[7] did a pioneering work in modeling the coalescence of two Lennard-Jones liquid droplets in a second immiscible fluid using MD simulations. The authors found that the coalescence of liquid droplets was completely driven by van der Waals and electrostatic interactions when the velocities of the droplets were small. The coalescence began when the molecules on the boundary of one droplet thermally drifted to the range of attraction of the other droplet and formed a string to attract both sides of the molecules.

Zhao and Choi[8] reported a MD study of the coalescence of 2 nm-sized water droplets in n-heptane, a system that is commonly encountered in the oil sands industry. Similarly, the coalescence process was initiated by the molecules at the edge of the clusters, which interacted with each other and formed a bridge between two clusters. Eventually, these molecules attracted and pulled out other molecules from their own respective cluster to interact with those from the other cluster. The authors made an important conclusion that the coalescence in n-heptane would occur only if the two droplets were very close to each other (~0.5 nm). If they were far apart (e.g., 1 nm), external driving forces should be applied.

In this paper, we present the computational results for pore formation and film rupture under external electric field obtained with a model, which we have designed to simulate the behavior of a toluene film immersed in a sodium chloride solution when an external electric field is applied perpendicularly to the film separating two water droplets. The electric field was increased in steps every 5 ns, which resembles a pulsed DC field. A comparison of the computed results can be made with the critical voltage values found in the experiment[6] having in mind the limitations—the computational results are for very thin films with no stabilizer in the emulsion. This model can be considered as a useful starting basis for a further study of the stability and the structure of thick emulsion films that are stabilized by indigenous crude oil surfactants, namely, asphaltenes, resins, and naphthenic acids.

II. THE MODEL AND SIMULATION PROCEDURE

To accurately simulate the interfacial phenomena, we have applied the classical MD method for *NVT* and *NPT* ensembles. Our previous experience has indicated that the ensemble choice is crucial for finding of coexisting structures in finite-size systems.[9] Since we are interested in the evolution of the film structure when an external electric field is applied, it has been natural to use different ensembles in MD simulations, which provide information on the molecular structure of the interface when the intermolecular potential is available.[10–12]

The model system is a 5 nm thick toluene film located perpendicularly to the z-axis of the simulation box. The size of the box, 24.8 × 24.8 × 24.8 nm, ensures that no artifacts will appear when 3*D* periodic boundary conditions are implemented to diminish finite-size effects. The box contains in total 1 028 400 atoms: 15 190 toluene molecules, 421 060 water molecules, and 2000 Na^+ and 2000 Cl^- ions. The force field parameters of the ions Na^+ and Cl^- are taken from *Gromos*96.[13] Parameters for toluene molecules are derived from benzyl side chain of the phenylalanine molecule. A three-site *SPC* (simple point charge) water model is used.[14]

Force fields usually divide non-bonded interactions into two: electrostatic interaction and van der Waals interaction. The particle mesh Ewald sum (PME-S) method was applied for handling the long range Coulomb interaction with the following cutoffs for truncation of the non-bonded potentials: $r_{coulomb}$ = 1.2 nm (for Coulomb interaction) and r_{vdw} = 1.0 nm (for van der Waals interaction). The surrounding dielectric constant was unity.

Large-scale molecular dynamics simulations of the model system are performed with the help of the *GROMACS* package, designed to simulate the Newtonian equations of motion for systems with hundreds to millions of particles.[15] The simulations are performed in *NVT* and *NPT* ensembles, which keep the total number of atoms constant; the temperature is kept at T = 298 K through a velocity rescaling thermostat. The velocity-rescaling thermostat is essentially a Berendsen thermostat, which can produce a correct canonical ensemble. In the *NVT* ensemble, the constant volume equals to the size of the simulation box, 24.8 × 24.8 × 24.8 nm. In the case of the *NPT* ensemble, the system is equilibrated at the constant pressure of 1 bar using the Parrinello-Rahman extended-ensemble pressure coupling (oscillatory relaxation), where the box vectors are subject to an equation of motion—as it is in the GROMACS package version 4.5.3.

In preliminary MD runs, the simulation time of 5 ns was determined to be sufficient for the thermodynamic equilibration of the total energy, pressure, and temperature of the model system.

An external electric field is applied in the z direction of the simulation box. In the *NVT* ensemble, the electric field strength is changed from 0 to 120 mV/nm in steps of 20 mV/nm, while in the *NPT* ensemble, the strength is changed from 0 to 75 mV/nm in steps of 25 mV/nm.

III. RESULTS AND DISCUSSION

A. *NVT* simulation—Build-up of interfacial charge

The interaction between the toluene film and the surrounding water molecules and ions results in a dynamic charge distribution. Fig. 1 illustrates the ion (sodium and chlorine) charge density distribution in the z-direction. The distribution is computed within the last 2.5 ns of the run (total run time 5 ns). The three curves correspond to 0, 60, and 100 mV/nm strengths of the external electric field. At 0 mV/nm (red curve), which calibrates the results, the charge fluctuates around zero at the film interfaces. A non-zero external field induces charge accumulation at the film interfaces. The curves for 60 mV/nm (green) and 100 mV/nm (blue) electric field strengths show

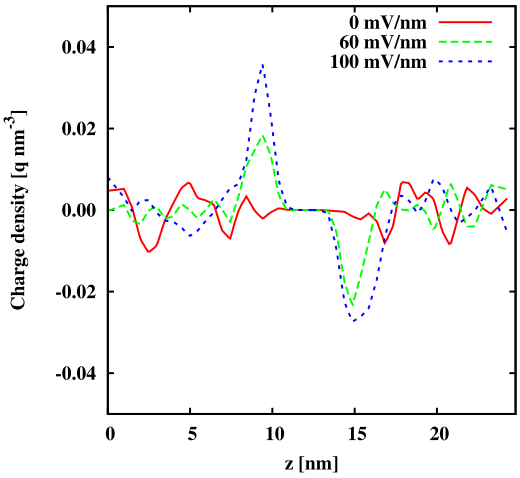

FIG. 1. Calculated free ion charge distribution in the z-direction demonstrates the build up of the interfacial charge with the applied field increase—0, 60, and 100 mV/nm.

that the accumulated charge increases with the field increase: one interface of the toluene film is charged positively due to the Na^+ ion accumulation, while the other interface is charged negatively due to the Cl^- ion accumulation. Thus, the emulsion film, subjected to the external electric field, resembles charging of a parallel-plate capacitor. At all applied fields, the total ion charge fluctuates around zero away from the film.

The time averaging was performed over the last 2.5 ns of the production run. Electric fields with strengths below

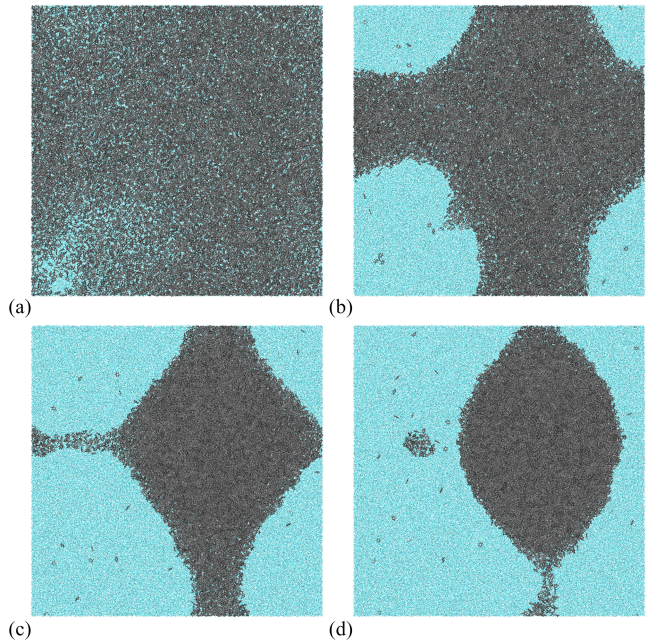

FIG. 3. Time evolution of the toluene film at an external electric field of 120 mV/nm; top view snapshots of the XY plane. (a) 500 ps, (b) 700 ps, (c) 1500 ps, and (d) 2000 ps.

100 mV/nm does not rupture the toluene film for the duration of the *NVT* simulation—5 ns. It should be noted that in the *NVT* ensemble, the charge distribution obtained at the 120 mV/nm field within time intervals less than 500 ps shown in Fig. 2(a) feature on average the same patterns as

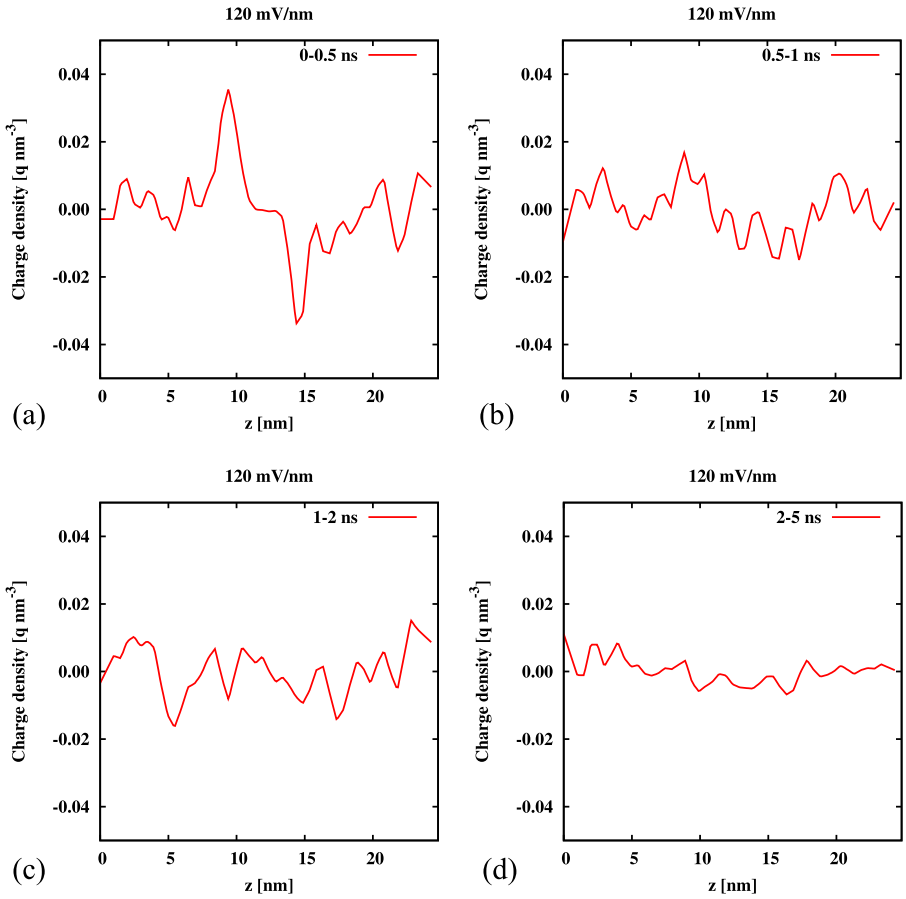

FIG. 2. Free ions charge distribution at 120 mV/nm (a) between 0 and 0.5 ns, (b) between 0.5 and 1 ns, (c) between 1 and 2 ns, and (d) between 2 and 5 ns.

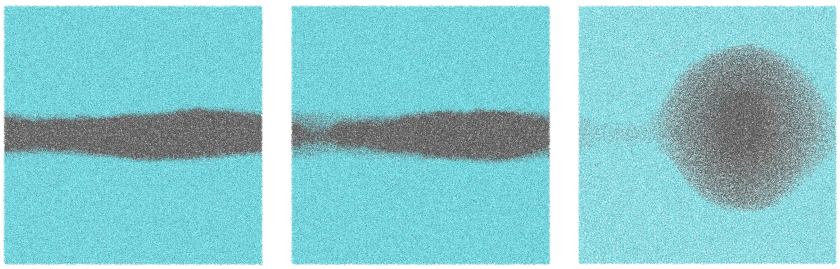

FIG. 4. Side view snapshots in the XZ plane for the 120 mV/nm external electric field applied perpendicularly to the toluene film: (a) the film profile after 100 ps; (b) startup of rupturing of the thinnest part of the film—between 400 ps and 500 ps; and (c) breakdown of the film and formation of a toluene drop at about 2000 ps.

the distribution computed at the 100 mV/nm field shown in Fig. 1.

The electric discharge is initiated after the pore formation as it is seen in Fig. 2(d). After 2 ns, the accumulated interfacial charge is drained, which is indicated with no peaks in the charge distribution of the ruptured film.

B. *NVT* simulation—Film rupture mechanism

When the electric field is set to 120 mV/nm, a pore is formed in the film after 500 ps. It is observed that the pore expands along the simulation box over time. The time evolution of the pore formation is shown in Fig. 3 for the time between 500 ps and 2000 ps. The pore is seen as a light spot in Fig. 3(a) at 500 ps. When the pore is wide enough water molecules fill in the pore area, seen as a bluish background in Fig. 3(b) at 700 ps. By observing the pore evolution in the toluene film, the time of the complete film rupture (formation of toluene drop) can be determined.

Inspection of the thickness profile at 120 mV/nm reveals the existence of a dimple inside the toluene film (Fig. 4(a)) prior to the film rupture. The role of the non-homogeneity has been widely reported in thin liquid film literature since 1941.[16]

Our simulations demonstrate that a non-homogeneous film ruptures at its thinnest place because the electric field strength is the highest there. In other words, the biconcave region of the film interface is subjected to a higher-than-average electrostatic pressure and therefore is a preferred site for the film rupture and nano-pore formation.

C. *NVT* simulation—The film structure

The charge density of free ions, water, and toluene molecules in the z-direction can be observed in Fig. 5. The figure illustrates the structure of the toluene film surrounded by aqueous electrolyte solution at 0, 60, 100, and 120 mV/nm electric field strengths. For the latter case, the density was averaged over the first 0.5 ns of simulation, i.e., before the startup of the rupturing process. The part of the film that contains only toluene molecules is called toluene *core*, and the *bulk* water phase is that part of the film, where the density of water molecules is maximal.

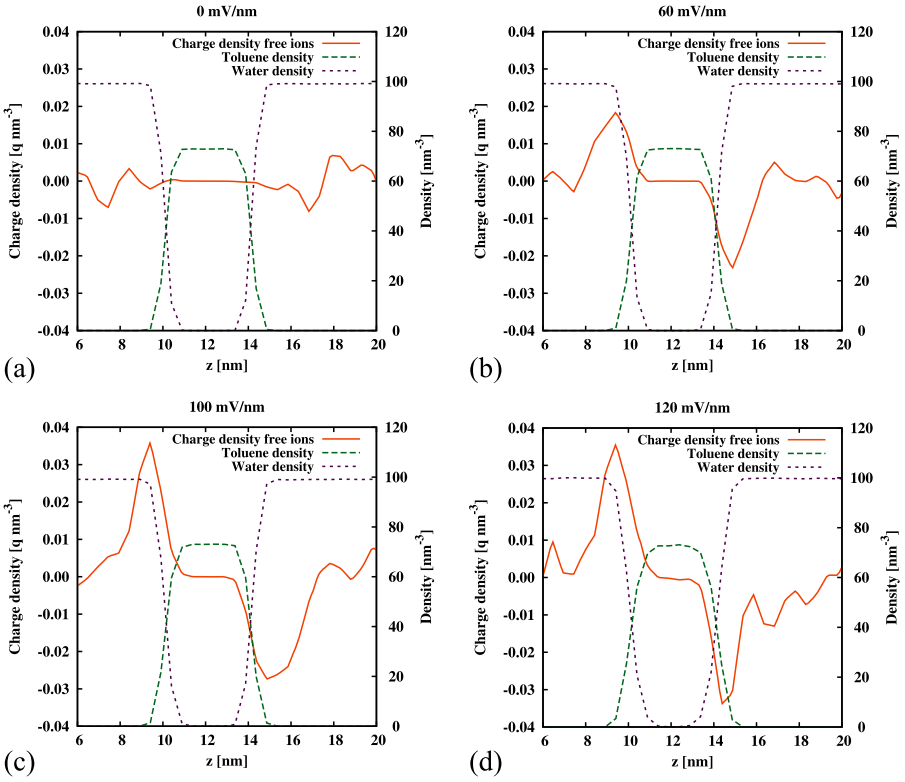

FIG. 5. Density distribution of free ions (red), toluene (green), and water molecules (purple) at different external electric fields in the *NVT* ensemble. (a) 0 mV/nm, (b) 60 mV/nm, (c) 100 mV/nm, and (d) 120 mV/nm.

TABLE I. Film thickness at different strengths of the applied electric field in the *NVT* ensemble.

Applied field	0 mV/nm	60 mV/nm	100 mV/nm	120 mV/nm
Toluene core (nm)	2.6	2.4	2.0	1.8
Interfacial layer (nm)	1.4	1.7	2.1	2.5
Total toluene layer (nm)	5.4	5.8	6.2	6.8

The core thickness was estimated using a double-sigmoid function Eq. (1) at 99% of the plateau height h, where x_0 and x_1 being the left and the right half-height, respectively, and a is the steepness of the sigmoid,

$$f(x; x_0, x_1, a, h) = h\frac{\exp^{-a(x-x_1)}}{(1+\exp^{-a(x-x_0)})^2}. \quad (1)$$

At no applied field, Fig. 5(a), there exists a pure toluene core of 2.6 nm thickness, which is surrounded by two interfacial layers formed by mixing toluene and water interfacial layers. In the toluene interfacial layer, the concentration of toluene molecules decreases in the direction from the pure toluene core toward the bulk water phases, eventually reaching zero concentration. In the aqueous interfacial layer, the concentration of water molecules decreases toward the toluene core. The toluene–water mixed layer is 1.4 nm thick, which is estimated as the distance where the toluene density in the z-direction drops from 99% to 1% from the plateau height h. The bulk aqueous phases contain Na^+ and Cl^- ions. The density profiles show that ions penetrate the mixed interfacial layers that border the toluene core. Thicknesses of the film core and the interfacial layer are shown in Table I.

Fig. 5(b) shows that the application of 60 mV/nm field leads to the build-up of accumulated positive charges on one side of the toluene film and negative charges on the other side. The peaks of accumulated charges are situated at the boundary between bulk water phase and the interfacial aqueous layer. In the direction toward the toluene core, the concentration of ions decreases and reaches zero at the toluene core. Ions penetrate only the mixed interfacial region, which is due to the formation of hydration shells. Fig. 5(c) reveals that the field increase up to 100 mV/nm is followed by the accumulation of more charges, bringing enough attractive force that leads to thinning of the pure toluene core by 0.6 nm down to 2.0 nm, while the thickness of the interfacial layers of toluene and water increases by 0.7 nm. A possible hypothesis is that the increased electrical compression reshapes the film topography making it a high amplitude rugged surface and the interfacial layer becomes thicker. Fig. 5(d) depicts the film structure (profile) at 120 mV/nm and data are averaged over the time interval of 500 ps. This is the moment (500 ps) just before the rupturing process takes place.

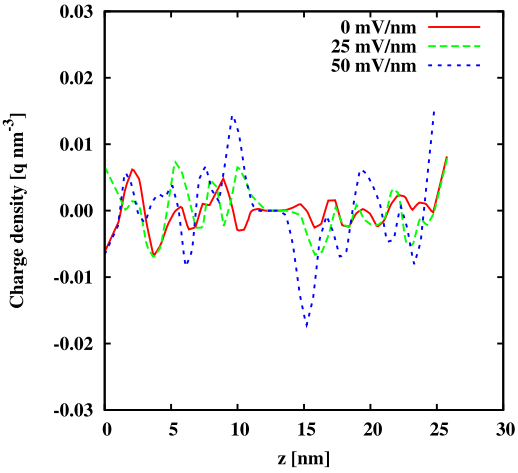

FIG. 6. Calculated charge of free ion density in the z-direction for three different external applied electric fields 0, 25, and 50 mV/nm in the case of the *NPT* ensemble.

The increase of potential from 100 to 120 mV/nm leads to additional thinning of the toluene core down to 1.8 nm. The thickness of interfacial layers of toluene and water increases by 0.4 nm.

D. *NPT* simulation—The film structure

This section presents the results obtained in the case of the *NPT* ensemble. The charge build-up is plotted in Fig. 6. Fig. 7 depicts the charge build-up at 0, 25 mV/nm, and 50 mV/nm. As in the *NVT* case, at zero external field, no peak formation is observed on both sides of the ionic line that exhibits zero-charge density. At 25 mV/nm such formation already takes place and becomes much pronounced at 50 and 75 mV/nm (Figure 7(c)). Film rupture occurs at a much lower electric field strength (75 mV/nm) compared to the *NVT* simulation (120 mV/nm). Film rupture occurs at a much lower electric field strength (75 mV/nm) compared to the *NVT* simulation (120 mV/nm). The information regarding the thickness of the

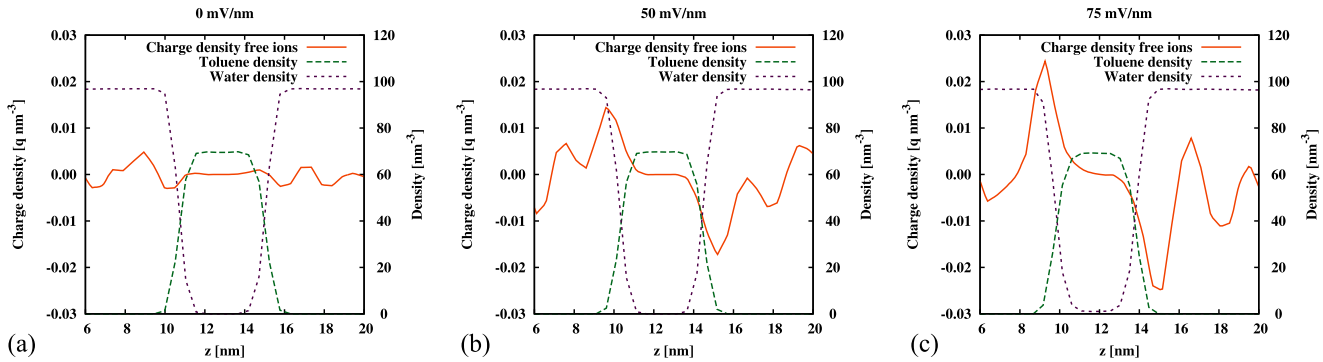

FIG. 7. Density distribution of free ions (red), toluene (green), and water molecules (blue) at different external electric fields in the *NPT* ensemble. (a) At no external electric field, 0 mV/nm, (b) at 50 mV/nm external electric field, and (c) at 75 mV/nm external electric field.

TABLE II. Film thickness at different strengths of the applied electric field in the *NPT* ensemble.

Applied field	0 mV/nm	50 mV/nm	75 mV/nm
Toluene core (nm)	2.6	2.2	1.8
Interfacial layer (nm)	1.8	2.0	2.4
Total toluene layer (nm)	6.2	6.2	6.6

toluene core, boundary layers, and the total film are summarized in Table II. The thickness of different layers was again determined by using the double-sigmoid formula in Eq. (1). At no applied field, the toluene core has the same thickness as in the NVT case. However, the difference between the two simulations is revealed in the size of the mixed boundary zone, being larger for the *NPT* ensemble. Increase of the electric field, as in the *NVT* case, again leads to thinning of the toluene core and to the expansion of the boundary layers. However, at 50 mV/nm (*NPT*) there is a bit higher thinning of the core, compared to 60 mV/nm (*NVT*), despite the lower applied field. This observation together with the obtained lower critical field could suggest enhanced development of instability in the *NPT* simulation. It should be noted that in both simulations at the critical field the core has the same thickness instants before the film rupture. Moreover, at that critical field the thickness of the boundary layers and the total layer is almost identical in both *NVT* and *NPT* ensembles. These observations—relevant from the point of view of the physical processes—prove the relevance of the model developed in this study.

IV. CONCLUSIONS

The results of MD simulations and their analysis offer insight into the intimate structure of the film, namely, the presence of a toluene core, neighboring a mixed boundary zone that contains altogether toluene and water molecules. The application of an external DC electric field leads to the redistribution of electrical charges and to the accumulation of oppositely charged ions (Na^+ and Cl^-) on both sides of the film. Thus, the behavior of the system resembles a liquid capacitor, whose charge increases with the rise of the external potential. In both *NVT* and *NPT* ensembles, *condenser plates*, where the charge density is maximal, are situated at the very border between the bulk aqueous (water) phase and the mixed layer. No ion penetration is observed within the toluene core, thus leaving all the distribution of charges within the mixed zone and the bulk phase, which could be attributed to the formation of hydration shells. When the critical electric field is reached, within a certain time after the field application, electric discharge occurs, indicating the beginning of the rupturing process. Visual snapshots of the evolution of the film area confirm the formation of a hole within the thinnest part of the initially non-homogeneous thin film.

The results clearly show that in *NPT* simulations, the critical instability is developed at much lower fields (75 mV/nm) than in NVT simulations (120 mV/nm). The first experimental investigation on the electro-induced rupture of real toluene-diluted bitumen emulsion films[6] shows that critical fields range between 4 and 11 mV/nm, depending on the bitumen concentration. Thus, the *NPT* simulation appears to be a better choice for further modeling of the systems that resemble more close the real films. In the *NPT* ensemble, we can expect that even lower values of the external electric field could rupture the toluene film if we prolong the simulation time. The compressive action of the build-up charges on both sides of the film is illustrated in the decrease of the thickness of the toluene core with the electric field. The behavior of the system resembles a capacitor with increasing charge with an increase of the external potential. However, in both types of simulations (*NVT* and *NPT*), the width of the mixed zone and hence of the total film increases with the field increase.

Moreover, the clarification of the detailed mechanism of the hole formation (wave-like or pore-like) and the role of thickness fluctuations on the rupturing process could be progressed through undertaking an extensive "subbox" thickness investigation, when the entire simulation box is divided into boxes along the xy-plane, as each one of them being analyzed.

In conclusion, we may argue that the model, we have developed for thin films, provides a ground for implementing a further complication of the investigated system, introducing surface active molecules, as well as a verification of our expectations for a decrease of the critical electric field when longer simulations are performed.

ACKNOWLEDGMENTS

S. Pisov and D. Dimova acknowledge the access to the HPC cluster in Sofia Tech Park (ERDF Project No. BG161PO003-1.2.05-0001-C0001), which was used for the heavy computations. S. Madurga acknowledges financial support from the Generalitat de Catalunya (Grant No. 2014-SGR-1251). The support of H2020 program of the European Union (project Materials Networking) is gratefully acknowledged by S. Madurga and M. Nedyalkova.

[1] C. F. Gardner and S. J. Buckner, "Separating and collecting particles of one liquid suspended in another liquid," U.S. patent 987115 A (21 March 1911).
[2] J. S. Eow and M. Ghadiri, Chem. Eng. J. **85**, 357 (2002).
[3] S. Mhatre, V. Vivacqua, M. Ghadiri, A. Abdullah, M. Al-Marri, A. Hassanpour, B. Hewakandamby, B. Azzopardi, and B. Kermani, Chem. Eng. Res. Des. **96**, 177 (2015).
[4] E. E. Isaacs and R. S. Chow, "Practical aspects of emulsion stability," in *Emulsions* (American Chemical Society, 1992), Chap. 2, pp. 51–77.
[5] M. R. Anklam, D. A. Saville, and R. K. Prud'homme, Colloid Polym. Sci. **277**, 957 (1999).
[6] N. Panchev, K. Khristov, J. Czarnecki, D. Exerowa, S. Bhattacharjee, and J. Masliyah, Colloids Surf., A **315**, 74 (2008).
[7] J. Koplik and J. R. Banavar, Science **257**, 1664 (1992).
[8] L. Zhao and P. Choi, J. Chem. Phys. **120**, 1935 (2004).
[9] A. Proykova, S. Pisov, and R. S. Berry, J. Chem. Phys. **115**, 8583 (2001).
[10] J. Koplik, S. Pal, and J. R. Banavar, Phys. Rev. E **65**, 021504 (2002).
[11] S. Razavi, J. Koplik, and I. Kretzschmar, Langmuir **30**(38), 11272 (2014).
[12] M. Nedyalkova, S. Madurga, S. Pisov, I. Pastor, E. Vilaseca, and F. Mas, J. Chem. Phys. **137**, 174701 (2012).
[13] W. R. P. Scott, P. H. Hnenberger, I. G. Tironi, A. E. Mark, S. R. Billeter, J. Fennen, A. E. Torda, T. Huber, P. Krger, and W. F. van Gunsteren, J. Phys. Chem. A **103**, 3596 (1999).
[14] H. J. C. Berendsen, J. R. Grigera, and T. P. Straatsma, J. Phys. Chem. **91**, 6269 (1987).
[15] H. J. C. Berendsen, D. van der Spoel, and R. van Drunen, Comput. Phys. Commun. **91**, 43 (1995).
[16] B. Derjaguin and L. Landau, Prog. Surf. Sci. **43**, 30 (1993).